Journal of Controlled Release 266 (2017) 109–118

Contents lists available at ScienceDirect

Journal of Controlled Release

journal homepage: www.elsevier.com/locate/jconrel

Intradermal vaccination with hollow microneedles: A comparative study of various protein antigen and adjuvant encapsulated nanoparticles

Guangsheng Du[a], Rania M. Hathout[a,b], Maha Nasr[a,b], M. Reza Nejadnik[a], Jing Tu[c], Roman I. Koning[d], Abraham J. Koster[d], Bram Slütter[a,e], Alexander Kros[c], Wim Jiskoot[a], Joke A. Bouwstra[a,*], Juha Mönkäre[a]

[a] Division of Drug Delivery Technology, Cluster BioTherapeutics, Leiden Academic Centre for Drug Research, Leiden University, Leiden, The Netherlands
[b] Department of Pharmaceutics and Industrial Pharmacy, Faculty of Pharmacy, Ain Shams University, Cairo, Egypt
[c] Department of Supramolecular & Biomaterials Chemistry, Leiden Institute of Chemistry, Leiden University, Leiden, The Netherlands
[d] Department of Molecular Cell Biology, Section Electron Microscopy, Leiden University Medical Center, Leiden University, Leiden, The Netherlands
[e] Division of Biopharmaceutics, Cluster BioTherapeutics, Leiden Academic Centre for Drug Research, Leiden University, Leiden, The Netherlands

ARTICLE INFO

Keywords:
Intradermal vaccination
Hollow microneedles
Nanoparticles
Antigen
Adjuvant

ABSTRACT

In this study, we investigated the potential of intradermal delivery of nanoparticulate vaccines to modulate the immune response of protein antigen using hollow microneedles. Four types of nanoparticles covering a broad range of physiochemical parameters, namely poly (lactic-*co*-glycolic) (PLGA) nanoparticles, liposomes, mesoporous silica nanoparticles (MSNs) and gelatin nanoparticles (GNPs) were compared. The developed nanoparticles were loaded with a model antigen (ovalbumin (OVA)) with and without an adjuvant (poly(I:C)), followed by the characterization of size, zeta potential, morphology, and loading and release of antigen and adjuvant. An in-house developed hollow-microneedle applicator was used to inject nanoparticle suspensions precisely into murine skin at a depth of about 120 μm. OVA/poly(I:C)-loaded nanoparticles and OVA/poly(I:C) solution elicited similarly strong total IgG and IgG1 responses. However, the *co*-encapsulation of OVA and poly (I:C) in nanoparticles significantly increased the IgG2a response compared to OVA/poly(I:C) solution. PLGA nanoparticles and liposomes induced stronger IgG2a responses than MSNs and GNPs, correlating with sustained release of the antigen and adjuvant and a smaller nanoparticle size. When examining cellular responses, the highest $CD8^+$ and $CD4^+$ T cell responses were induced by OVA/poly(I:C)-loaded liposomes. In conclusion, the applicator controlled hollow microneedle delivery is an excellent method for intradermal injection of nanoparticle vaccines, allowing selection of optimal nanoparticle formulations for humoral and cellular immune responses.

1. Introduction

Skin is an attractive administration site for immunization and may act as an excellent alternative for traditional intramuscular or subcutaneous vaccination. Furthermore, intradermal vaccination may enable dose sparing, since the skin has a rich network of immune cells compared to muscle or subcutaneous tissue [1]. However, the uppermost layer of the skin, the stratum corneum, is the main barrier that prevents the transport of vaccines (> 500 Da) across the skin. Therefore, novel delivery methods need to be developed. Among various methods developed for antigen delivery *via* the skin, especially microneedle-based approaches have recently attracted increasing attention [2]. The major advantage of microneedles is their ability to pierce the skin in a minimally invasive manner and subsequently deliver their payload in the superficial skin layers potentially without pain, owing to the limited penetration depth of microneedles (typically < 500 μm) [3].

Several microneedle types have been developed for vaccine delivery, such as coated or dissolving microneedles which can release the dry antigen into the epidermis and dermis after the piercing of the skin [2]. In contrast, hollow microneedles can be used to deliver antigens or particulate formulations as solutions or suspensions into the skin. To this end, in our group a hollow microneedle device has been developed that allows precise and controlled injections into the epidermis and dermis by using etched fused-silica capillary-based microneedles [4–6]. The advantage of the hollow microneedles compared to dissolving or coated microneedles is that little time is required for modifying the dose, formulation or administration depth. This is particularly

* Corresponding author.
E-mail address: bouwstra@lacdr.leidenuniv.nl (J.A. Bouwstra).

http://dx.doi.org/10.1016/j.jconrel.2017.09.021
Received 6 July 2017; Received in revised form 12 September 2017; Accepted 13 September 2017
Available online 21 September 2017

advantageous when studying optimization of formulations or parameters for the immunization (*e.g.* penetration depth or vaccine dose). Furthermore, if required, a higher dose can be injected into the skin compared to dissolving and coated microneedles.

Subunit antigens are based on purified antigens and are regarded safer than traditional whole bacterium- or virus-based vaccines [7]. However, these antigens have often lower immunogenicity and therefore adjuvants, such as toll-like receptor (TLR) ligands or toxoids, are needed to increase the immune response [8]. Recently, nanoparticles have gained growing attention for the delivery of subunit vaccines because of their capability of protecting antigens from degradation, forming a depot at the site of injection, and facilitating antigen uptake by dendritic cells (DCs) [9–11]. Studies have additionally shown that co-formulation of antigen and adjuvant into a nanoparticle might be crucial to improve immune responses against subunit vaccines [12–15]. However, it is not well understood how the physicochemical properties such as size, material, surface charge or release behavior of antigen/adjuvant influence the immune response. Previously, it has been proposed that positively charged nanoparticles with a size smaller than about 200 nm might be optimal for the interaction with antigen-presenting cells [9,16–18]. Moreover, sustained release of antigen and adjuvant from nanoparticles and a depot effect of nanoparticles on the cell surface could allow the co-delivery of antigen and adjuvant to antigen-presenting cells [17,19]. However, most vaccination studies have been performed by intramuscular or subcutaneous injection and no studies have directly compared different nanoparticles for intradermal vaccine delivery.

The aim of this study was to assess the potential of antigen loaded nanoparticles, with or without co-encapsulated adjuvant, to induce humoral and cellular immune responses after hollow microneedle-mediated intradermal immunization. To this end, we prepared four different nanoparticulate delivery systems with varying physicochemical properties, namely poly (lactic-*co*-glycolic) acid (PLGA) nanoparticles, liposomes, mesoporous silica nanoparticles (MSNs) and gelatin nanoparticles (GNPs). PLGA nanoparticles [10,20–24] and liposomes [12,18,22,25] have been extensively investigated as biocompatible and biodegradable nanoparticle vaccine delivery systems. MSNs gain increasing attention for vaccine delivery because of their controlled size and mesostructure, excellent *in vivo* biocompatibility and high loading capacity [26,27]. Gelatin based nanoparticles have been studied as promising vaccine carriers because of their excellent biocompatibility, stability and aptness for surface modification [28–30].

A model antigen, ovalbumin (OVA), with and without a TLR3 agonist, poly(I:C), was encapsulated into the nanoparticles. First, the physicochemical properties and the *in vitro* release of antigen and adjuvant of the different nanoparticulate formulations were characterized. Next, mice were immunized with the formulations by using a hollow microneedle device followed by the analysis of humoral and cellular immune responses. The results reveal that the immune response depends on encapsulation of antigen/adjuvant and the characteristics of nanoparticles. Furthermore, we demonstrate that the hollow microneedles together with the applicator are excellent tools for intradermal vaccination and screening of nanoparticulate formulations.

2. Materials and methods

2.1. Materials

PLGA (acid terminated, lactide glycolide 50:50, Mw 24–38 kDa), gelatin from porcine skin (bloom 300), OVA for *in vitro* studies (albumin from chicken egg white, lyophilized), bovine serum albumin (BSA) ≥ 96%, gluteraldehyde, glycine, cholamine chloride hydrochloride (2-aminoethyl)-trimethylammoniumchloride hydrochloride, 1-ethyl-3-(3-dimethyl-aminopropyl) carbodiimide hydrochloride (EDC), cholesterol (≥ 99%) and hydrofluoric acid ≥ 48% were purchased from Sigma-Aldrich (Zwijndrecht, The Netherlands). Polyvinyl alcohol (PVA) 4–88 (31 kDa) and ethylenediaminetetraacetic acid (EDTA) were purchased from Fluka (Steinheim, Germany). 1-step™ ultra 3,3′,5,5′-tetramethylbenzidine (TMB) was obtained from Thermo-Fisher Scientific (Waltham, MA). Endotoxin-free OVA, polyinosinic-polycytidylic acid (poly(I:C)) (low molecular weight) and its rhodamine-labeled version were purchased from Invivogen (Toulouse, France). Egg phosphatidylcholine (EggPC), 1,2-dioleoyl-*sn*-glycero-3-phosphocholine (DOPC), 1,2-dioleoyl-*sn*-glycero-3-[phosphor-L-serine](sodium salt) (DOPS), 1,2-dioleoyl-3-trimethylammonium-propane chloride salt (DOTAP) and 1,2-dioleoyl-*sn*-glycero-3-phosphoethanolamine (DOPE) were ordered from Avanti Polar Lipids (Alabaster, AL). HRP-conjugated goat anti-mouse total IgG, IgG1 and IgG2a were purchased from Southern Biotech (Birmingham, AL). Fluorescently labeled antibodies specific for CD4, CD8 and CD45.1 were ordered from eBioscience (San Diego, The Netherlands). Sulfuric acid (95–98%) was obtained from JT Baker (Deventer, The Netherlands). Ethyl acetate and silicone oil (AK350) were ordered from Boom Chemicals (Meppel, The Netherlands). Dimethylsulfoxide (DMSO) was ordered from Biosolve BV (Valkenswaard, The Netherlands). Sodium dodecyl sulfate (SDS) was purchased from Merck Millipore (Hohenbrunn, Germany). Vivaspin 2 centrifugal concentrators (PES membrane, MWCO 1000 kDa) were obtained from Sartorius Stedim (Nieuwegein, The Netherlands). Sterile phosphate buffered saline (PBS, 163.9 mM Na^+, 140.3 mM Cl^-, 8.7 mM HPO_4^{2-}, 1.8 mM H_2PO^{4-}, pH 7.4) was obtained from Braun (Oss, The Netherlands). Cell culture medium was prepared by mixing Roswell Park Memorial Institute medium (RPMI) with 10% Fetal bovine serum (FBS), 1% L-glutamine and 1% Penicillin-streptamycin. 1 mM phosphate buffer (PB, 0.77 mM Na_2HPO_4, 0.23 mM NaH_2PO_4, pH 7.4), 10 mM PB (7.7 mM Na_2HPO_4, 2.3 mM NaH_2PO_4, pH 7.4), 5 mM 4-(2-hydroxyethyl)piperazine-1-ethanesulfonic acid (HEPES, pH 7.4) buffer, lysis buffer (150 mM ammonium chloride, 10 mM $KHCO_3$, 0.1 mM EDTA, pH 7.2), and FACS buffer (2% FBS in PBS, pH 7.4) were prepared in the lab. All the other chemicals used are of analytical grade and Milli-Q water (18 MΩ/cm, Millipore Co.) was used for the preparation of all solutions.

2.2. Preparation of nanoparticles

2.2.1. Preparation of PLGA nanoparticles

OVA loaded PLGA nanoparticles (PLGA-OVA) were prepared by double emulsion with solvent evaporation method as previously reported with modifications [31]. Briefly, 75 μl OVA (20 mg/ml) in PBS was dispersed in 1 ml ethyl acetate containing 25 mg/ml PLGA by using a Branson sonifier 250 (Danbury, CT) for 15 s with a power of 20 W. The obtained water-in-oil emulsion was emulsified with 2 ml aqueous solution containing 2% (w/v) PVA with the sonifier (15 s, 20 W). The water-in-oil-in-water double emulsion was added dropwisely into 25 ml 0.3% (w/v) PVA (40 °C) under stirring. The ethyl acetate was evaporated by a rotary evaporator (Buchi rotavapor R210, Flawil, Switzerland) for 3 h (150 mbar, 40 °C). The nanoparticles were collected by centrifugation (Avanti™ J-20XP centrifuge, Beckman Coulter, Brea, CA) at 35000 *g* for 10 min. Finally, they were washed twice with 1 mM PB to remove the excess OVA and PVA and dried in an ice condenser (Alpha 1–2, Osterode, Germany) in freeze vacuum (− 49 °C, 90 mbar) overnight for further use and storage.

To prepare OVA and poly(I:C) co-encapsulated PLGA nanoparticles (PLGA-OVA-PIC), 18.75 μl OVA (40 mg/ml) and 75 μl poly(I:C) (46.7 mg/ml, including 0.03% fluorescently labeled equivalent) were emulsified with 1 ml PLGA (25 mg/ml) in ethyl acetate to obtain the water-in-oil emulsion. The rest of the procedure was identical to that of PLGA-OVA.

2.2.2. Preparation of liposomes

Liposomes were prepared by a film hydration method [32]. A thin lipid film of EggPC: DOPE: DOTAP in a molar ratio of 9:1:2.5 was

created by evaporating chloroform of lipid stock solutions (25 mg/ml) using a rotary evaporator (Buchi rotavapor R210, Flawil, Switzerland). To prepare OVA loaded liposomes (Lipo-OVA), the lipid film was rehydrated in 10 mM PB (pH 7.4) containing 0.25 mg/ml OVA, and subsequently stabilized at room temperature for 1 h, resulting in final lipid concentration of 12.5 mg/ml. In the case of OVA and poly(I:C) co-encapsulated liposomes (Lipo-OVA-PIC), after lipid film hydration, 250 μl poly(I:C) solution (1.32 mg/ml, containing 0.5% rhodamine-labeled poly(I:C)) was added slowly (2 μl/min) by using a syringe pump to the liposome suspension under stirring. Finally, the liposomes were extruded (LIPEX™ extruder, Northern Lipids, Burnaby, Canada) four times through a carbonate filter with a pore size of 400 nm and another four times through a filter with a pore size of 200 nm (Nucleopore Millipore, Amsterdam, The Netherlands). The obtained suspensions were transferred into VivaSpin 2 centrifuge concentrators (1000 kDa MWCO) and centrifuged (Allegra X-12R, Beckman Coulter, Indianapolis, IN) twice for 7–8 h (350 *g*, 22 °C) to remove the excess OVA and poly(I:C) [18]. The liposome suspensions were collected and stored at 4 °C until further use.

2.2.3. Preparation of MSNs

Large pore MSNs were synthesized and used for the loading of antigen and adjuvant as described earlier [33]. To improve the colloidal stability of antigen loaded MSNs, negatively charged liposomes were fused to the surface of MSNs, as reported previously [34,35]. For this purpose liposomes were prepared by dispensing stock solutions of DOPC (70 μl, 25 mg/ml), DOPS (20 μl, 12.5 mg/ml) and cholesterol (10 μl, 25 mg/ml) in chloroform into scintillation vials. A lipid film was created by slow evaporation of chloroform in the vial under a nitrogen flow and dried in vacuum overnight. The lipid film was rehydrated by the addition of 1 ml of 1 mM PB (pH 7.4) and the mixture was vortexed for 10 s to form a cloudy lipid suspension. The obtained suspension was sonicated in a water bath for 10 min. The resulting clear liposome dispersions were stored at 4 °C for further use.

To prepare lipid bilayer coated and OVA encapsulated MSNs (LB-MSN-OVA), OVA (0.5 ml, 0.25 mg/ml) in 1 mM PB (pH 7.4) was first transferred into a 2 ml micro-centrifuge tube, followed by the addition of MSNs (0.5 ml, 1 mg/ml) and liposomes (0.5 ml, 2 mg/ml). For OVA and poly(I:C) co-encapsulated and lipid coated MSNs (LB-MSN-OVA-PIC), 0.5 ml solution containing 0.25 mg/ml OVA and 0.094 mg/ml poly(I:C) (containing 1.2% rhodamine-labeled poly(I:C)) were mixed with MSNs and liposomes similarly to LB-MSN-OVA. The resulting mixtures were incubated for 1.5 h under shaking (400 rpm, 25 °C). The nanoparticles were collected and excess liposomes, OVA and poly(I:C) were removed by centrifuging the sample (9000 *g*, 5 min) with a Sigma 1–15 centrifuge (Osterode, Germany). The obtained nanoparticles were stored at 4 °C before the use.

2.2.4. Preparation of GNPs

GNPs were prepared by using a two-step desolvation method as previously described [36]. First, 1.25 g gelatin (cationic, pI 7–9) was dissolved in 25 ml ultrapure water at 50 °C while stirring at 600 rpm for 30 min. The first desolvation step was carried out by addition of 25 ml acetone. The mixture was left for 1 h until the gelatin precipitated. The supernatant was discarded and the sediment was re-dissolved in 25 ml ultrapure water at 50 °C while stirring at 250 rpm for 30 min. Subsequently, the pH of the solution was adjusted to 2.5 by using concentrated HCl and a second desolvation step was performed by dropwise (0.1 ml/s) addition of 80 ml acetone at 50 °C while stirring at 1200 rpm. The crosslinking of the GNPs was accomplished by adding 25 (w/w)% glutaraldehyde (GA) solution. The amount of added GA was adjusted such that the molar ratio between the NH_2 groups of gelatin and GA molecules was 1:1. Calculations were performed based on the assumptions that $MW_{gelatin}$ = 100 kDa and 1 mol gelatin has 37 mol NH_2 [36]. The resultant suspension was stirred at 600 rpm for 16 h at room temperature. Next, an equal volume of 100 mM glycine solution was added to the suspension to block the unreacted GA and stop the cross-linking reaction. The suspension was stirred for 1 h at room temperature before being centrifuged at 7000 *g* for 1 h (Avanti™ J-20XP centrifuge, Beckman Coulter, Brea, CA) to separate the GNPs from the reaction mixture. The GNPs were rinsed with ultrapure water in three rounds of centrifugation and resuspension. The obtained GNPs were cationized to increase the positive surface charge and consequently enhance the loading of OVA and poly(I:C). Briefly, the pH of GNP suspension was adjusted to 4.5 and the quaternary amine cholamine (10% of the weight of GNPs) was added under constant stirring. After 5 min, EDC (10% of the weight of GNPs) was added to the suspension to activate the carboxylic groups of gelatin which would couple cholamine. The mixture was stirred for 3 h at room temperature. The cationized GNPs were purified by three successive centrifugation steps as described above. Finally, the nanoparticles were resuspended in ultrapure water by using vortexing and probe sonication [37], and stored at 4 °C for further experiments.

To prepare OVA loaded GNPs (GNP-OVA) for the humoral response study, 100 μg OVA in water was added to 2000 μg GNPs in water (total volume 1 ml) and the samples were mixed for 1 h (400 rpm, 25 °C). For OVA and poly(I:C) co-loaded GNPs (GNP-OVA-PIC), after shaking OVA and GNPs for 1 h, 100 μg poly(I:C) (containing 1% rhodamine-labeled poly(I:C)) was added to the GNP suspension and the suspension was mixed for another 1 h. Finally, the loaded nanoparticles were separated by centrifugation at 2800 *g* for 5 min, followed by re-suspension in deionized water. For the cellular response study, a modification of the method was required to allow administration of a higher dose. Instead of water, 4 mM HEPES buffer (pH 7.4) was used for loading to control the pH. For GNP-OVA the added amounts of GNPs and OVA were 6000 μg and 300 μg (in 1.5 ml), respectively, and for GNP-OVA-PIC, the amounts of GNP, OVA and poly(I:C) were 7000 μg, 200 μg and 200 μg (in 1.5 ml), respectively. The modification did not significantly change the characteristics of nanoparticles.

2.3. Characterization of the nanoparticles

2.3.1. Particle size and zeta potential determination

The particle size and polydispersity index (PDI), and zeta potential for all formulations were determined by dynamic light scattering and laser doppler velocimetry, respectively, by using a Nano ZS® zetasizer (Malvern Instruments, Worcestershire, U.K.). Particle size measurements were performed in 10 mM PB (pH 7.4) (PLGA nanoparticles, liposomes and MSNs) or ultrapure water (GNPs), while for zeta potential measurements samples were diluted in 5 mM HEPES buffer (pH 7.4).

2.3.2. Morphological characterization

Morphology of PLGA nanoparticles and GNPs was visualized by using scanning electron microscopy (SEM, Nova NanoSEM, FEI, Eindhoven, The Netherlands) with a voltage of 15 kV. Nanoparticles were first freeze-dried and coated with a thin layer of carbon. MSNs were visualized by transmission electron microscopy (TEM) using a JEOL 1010 instrument (JEOL Ltd., Peabody, MA) with an accelerating voltage of 70 kV. To prepare the samples, several droplets of MSN suspension (1 mg/ml) were added on a copper grid, dried overnight and coated with carbon. Liposomes were visualized by Cryo-EM. The samples were diluted to 5 mg/ml and drops of 3 μl were applied to 300 mesh EM grids with lacey carbon (Ted Pella, USA). Grids were transferred into an electron microscopy grid plunger (EM GP, Leica, Germany) operated at room temperature and 100% humidity. The sample was vitrified by removing excess liquid immediately followed by plunging into liquid ethane and the plunge-frozen grids were stored in liquid nitrogen until further use. Samples were inserted into a Gatan 626 cryo holder (Gatan, Pleasanton, CA). A Tecnai F20 microscope (Thermo-Fisher, Eindhoven, The Netherlands) was operated at 200 kV and the EM images were recorded at defocus values between 1 and 3 μm underfocus on a Gatan 4 k × 4 k CCD (Gatan, Germany).

2.3.3. Determination of loading efficiency of OVA and poly(I:C)

To determine the loading efficiency of OVA and poly(I:C) in PLGA nanoparticles, the nanoparticles were dissolved in a mixture of 15% (v/v) DMSO and 85% (v/v) 0.05 M NaOH and 0.5% SDS. The amount of OVA was quantified by the microBCA method following the manufacturer's instructions. The amount of poly(I:C) was determined by the fluorescence intensity of rhodamine labeled poly(I:C) (λ_{ex} 545 nm/λ_{em} 576 nm) with a plate reader (Tecan M1000, Männedorf, Switzerland). The loading efficiency of OVA in liposomes, MSNs and GNPs was determined by measuring its intrinsic fluorescence intensity (λ_{ex} 280 nm/λ_{em} 320 nm) with the Tecan M1000 plate reader in the supernatant before and after the encapsulation (MSNs and GNPs) or in the purification filtrates (liposomes). The loading efficiency of poly(I:C) in these nanoparticles was quantified similarly by measuring the fluorescence of its rhodamine labeled equivalent (λ_{ex} 545 nm/λ_{em} 576 nm).

The encapsulation efficiency (EE) and loading capacity (LC) of OVA and poly(I:C) in the nanoparticles were calculated as below:

$$EE\% = \frac{M_{loaded\ OVA/poly(I:C)}}{M_{total\ OVA/poly(I:C)}} \times 100\% \quad (1)$$

$$LC\% = \frac{M_{loaded\ OVA/poly(I:C)}}{M_{nanoparticles+OVA+poly(I:C)}} \times 100\% \quad (2)$$

where $M_{loaded\ OVA/poly(I:C)}$ represents the mass of loaded OVA or poly(I:C), $M_{total\ OVA/poly(I:C)}$ is the total amount of OVA or poly(I:C) added to the formulations and $M_{nanoparticles\ +\ OVA\ +\ poly(I:C)}$ is the total weight of nanoparticles, OVA and poly(I:C).

2.3.4. In vitro release studies

To study the release of OVA and poly(I:C), the nanoparticles were dispersed in PBS and shaken by using an Eppendorf thermomixer (Nijmegen, The Netherlands) at 37 °C with a speed of 550 rpm. The concentration for PLGA nanoparticles, liposomes, MSNs and GNPs after the suspension was 3 mg/ml, 5 mg/ml (lipid concentration), 1 mg/ml and 1.3 mg/ml, respectively. At predetermined time intervals, the tubes were taken out of the shaker bath and centrifuged at 10000 *g* for 10 min (PLGA nanoparticles and MSNs) or at 2800 *g* for 5 min (GNPs). A release sample of 600 μl was taken from the supernatant and replaced by fresh release medium. In the case of liposomes, 300 μl sample was collected to Vivaspin 500 concentrators. After the centrifuging (350 *g*, 30 min), the filtrate was collected and replaced with fresh medium. The amount of released OVA and poly(I:C) were determined by intrinsic fluorescence of OVA (λ_{ex} 280 nm/λ_{em} 320 nm) and fluorescence of rhodamine labeled poly(I:C) (λ_{ex} 545 nm/λ_{em} 576 nm), respectively, using a Tecan M1000 plate reader. The amount of released OVA in PLGA nanoparticles was determined by the MicroBCA method.

2.4. Hollow microneedles and applicator

Hollow microneedles were prepared as described earlier [38]. Briefly, 4-cm pieces of polyimide-coated fused silica capillaries (Polymicro, Phoenix AZ, 375 μm outer diameter, 50 μm inner diameter) were first filled with silicone oil in a vacuum oven (100 °C) overnight and subsequently etched for 4 h in ≥ 48% hydrofluoric acid. The polyimide coating was removed from the etched ends of capillaries by dipping them into heated (250 °C) sulfuric acid for 5 min.

A hollow-microneedle applicator was used to control the injection depth and volume as previously reported [5]. A 100-μl syringe with an inner diameter of 1.46 mm was used in conjunction with a syringe pump (NE-300, Prosense, Oosterhout, The Netherlands) and silica capillaries. High-pressure resistant CapTite™ connectors were used to connect the pump, syringe, capillaries and needles.

2.5. Immunization studies

Female BALB/c mice ($H2^d$) and C57BL/6 mice ($H2^b$) were used for the antibody response and T-cell response study, respectively. The mice were 7–8 weeks old at the beginning of the experiment. All the mice were purchased from Charles Rivers (Maastricht, The Netherlands) and were housed under standardized conditions in the animal facility of Leiden Academic Centre for Drug Research of Leiden University. Experiments were approved by the ethical committee on animal experiments of Leiden University (Licence number 14176).

2.5.1. Antibody response study

BALB/c mice were anesthetized by intraperitoneal injection of ketamine (60 mg/kg) and xylanize (4 mg/kg), which was followed by the shaving of the injection site. At the same day mice (n = 8/group) were immunized by an intradermal injection of 10 μl nanoparticles loaded with 0.31 μg OVA, with or without approximately 0.31 μg poly(I:C), on the flank of the mouse by using the applicator, as described above. Solutions of 0.31 μg OVA, with or without 0.31 μg poly(I:C), were used as controls. The injection depth was set to about 120 μm. In addition, subcutaneous injection of 0.31 μg OVA (100 μl) was used as another control. Mice were immunized on day 0 (prime), day 21 (1st boost) and day 42 (2nd boost), and sacrificed on day 49. Before each immunization, on the same day, a venous blood sample was collected from the tail to measure the antibody responses. Before the sacrifice, the blood sample was collected from the femoral artery.

2.5.2. T cell response study

OT-I (OVA-specific $CD8^+$) and OT-II (OVA-specific $CD4^+$) T cell transferred C57BL/6 mice were used for the T cell response study. To obtain OT-I and OT-II T cells, spleens of OT-I and OT-II transgenic mice (CD45.1) were isolated and single cell suspensions were obtained by forcing the spleens through a 70 um strainer. After erythrocyte depletion with ammonium chloride, percentage of $CD8^+$/$Valpha2^+$ or $CD4^+$/$Valpha2^+$ cells was determined by flow cytometry (BD FACSCanto-II, San Jose, CA). An equivalent of 8000 OT-I and 56,000 OT-II cells were intravenously transferred through the tail vein into C57BL/6 mice. Next day, the T cell transferred mice were immunized with nanoparticle formulations. OVA and poly(I:C) solutions were used as controls. Before the immunization, mice were anesthetized by isoflurane inhalation (induction 4–5% and maintenance 1%), which was followed by shaving of the injection site. On the same day, mice (n = 5/group) were immunized by three intradermal injections of 13.3 μl (totally 40 μl) formulation containing 5 μg OVA with or without approximately 5 μg poly(I:C) on the flank of the mouse (two injections on the right side, one injection on the left side) by using the hollow-microneedle applicator as described above. 7 days after the immunization, venous blood sample was collected from the tail to analyze the T cell response.

2.6. Determination of OVA specific IgG antibodies

OVA-specific antibodies were analyzed by a sandwich enzyme-linked immunosorbent assay (ELISA) as described earlier [39]. Briefly, wells of the 96 well-plates were first coated with 500 ng OVA for 1.5 h at 37 °C. The plates were blocked by incubation with 1% (w/v) BSA for 1 h at 37 °C. After the blocking, appropriate three-fold serial dilutions of mouse sera were applied to the plates and incubated for 1.5 h at 37 °C. Then the plates were incubated with horseradish peroxidase-conjugated goat antibodies against IgG, IgG1 and IgG2a (1:5000 dilution) for 1 h at 37 °C. Finally, specific antibodies were detected by TMB. The absorbance was measured at 450 nm (Tecan M1000) and the antibody titer was determined as a log10 value of the mid-point dilution of S-shaped dilution-absorbance curve of the diluted serum level.

2.7. $CD4^+$ and $CD8^+$ T cell responses

The erythrocytes of the blood sample (100 μl) were first lysed by incubating samples with 3 ml lysis buffer for 6 min in ice, followed by

addition of 5 ml cell culture medium. After the centrifugation (5 min, 500 *g*), the supernatant was discarded and the samples were suspended in 5 ml FACS buffer. Next, samples were centrifuged and 200 μl of cell suspension was added to the 96-well plate after discarding the supernatant. The cell surfaces were stained by incubating the cells with 100 μl diluted (1:800) fluorescently labeled antibodies specific for CD45.1 (eFluor450), CD4 (APC) and CD8α (PerCP) for 30 min (100 μl/well). After 30 min incubation at 4 °C, the excess antibodies were washed by using FACS buffer. The cells were incubated with fixation and permeabilization solution (BD Biosciences) for 10 min at 4 °C. Finally, the cells were washed with FACS buffer and analyzed by flow cytometry (BD FACSCanto-II, San Jose, CA). The data were analyzed by using FlowJo software.

2.8. Statistical analysis

All the data of immunization studies were analyzed by one way ANOVA with Bonferoni's post-test by using GraphPad Prism software (version 5.02). The level of significance was set at $p < 0.05$.

3. Results

3.1. Physicochemical characterization of nanoparticles

Four different nanoparticle formulations (PLGA nanoparticles, liposomes, MSNs and GNPs) were developed and characterized in terms of size, zeta potential, surface morphology, and loading and release properties of encapsulated antigen and adjuvant. Physicochemical characteristics of the nanoparticles are summarized in Table 1. According to DLS, PLGA nanoparticles and liposomes had an average diameter between 120 nm and 170 nm with a PDI value below 0.1 (PLGA nanoparticles) and 0.3 (liposomes). MSNs and GNPs had a larger diameter, ranging from 500 nm to 760 nm, and PDI values between 0.1 and 0.3. The electron microscopy images revealed a spherical shape of PLGA nanoparticles, liposomes and GNPs, whereas MSNs had a rectangular shape with mesochannels along the short axis (Fig. 1). The estimated size based on electron microscopy images is consistent with the size in Table 1 for PLGA nanoparticles and liposomes. MSNs had a smaller particle size in TEM images than in DLS measurements, indicating the presence of aggregates in these nanoparticle suspensions. In the case of GNPs, particles are swelling in aqueous medium [40], which may explain the smaller particle size in SEM images as compared to DLS.

PLGA nanoparticles and MSNs had a negative zeta potential, whereas liposomes and GNPs possessed a positive zeta potential. In general, *co*-encapsulation of poly(I:C) did not substantially affect the size, the PDI and zeta potential of the nanoparticles (Table 1). Moreover, both OVA and poly(I:C) were efficiently encapsulated into the nanoparticles. The EE% of OVA reached > 60% for all nanoparticles except LB-MSN-OVA-PIC (34%) (Table 1). Similarly, poly(I:C) had a EE % higher than 60%, except for PLGA nanoparticles (13.9%). During the development of the preparation process of the nanoparticles, the introduced amounts of antigen and adjuvant were optimized to obtain similar loading capacities of OVA and poly(I:C) for each delivery system (Table 1).

3.2. In vitro release of OVA and poly(I:C) from nanoparticles

To determine the release properties of OVA or poly(I:C) from the nanoparticles, the particles were dispersed in PBS and the released amount of OVA or poly(I:C) was measured at regular time intervals during one month (Fig. 2). PLGA nanoparticles slowly released OVA and on day 30, approximately 13% and 20% of the encapsulated OVA were released from PLGA-OVA and PLGA-OVA-PIC, respectively. Poly (I:C) release followed the OVA release and approximately 20% of the encapsulated poly(I:C) was released during one month. Liposomes released about 30% OVA on the first day, followed by a slow release to 40% during one month. Approximately 12% poly(I:C) was slowly released from liposomes during one month. MSNs showed a burst release of approximately 40% OVA within the first 6 h, followed by a slower and linear release phase from 40% to almost 100% in the subsequent two weeks. The release of poly(I:C) was slower and only 30% poly(I:C) was released from LB-MSN-OVA-PIC within 15 days. GNPs showed a burst release of nearly all loaded OVA and poly(I:C) within 2 h, followed by a slow release until 4 days.

3.3. Antibody responses after intradermal immunization

First, it was examined whether intradermal vaccination with solutions or nanoparticles containing 0.31 μg OVA with or without poly(I:C) (~0.31 μg) (Table 1) can induce antigen specific antibodies. The dose of antigen was chosen based on a dose response study (data not shown). As shown in Fig. 3, all groups, except the subcutaneous control of OVA solution, showed a detectable total IgG response on day 21, and the highest response was detected for the PLGA-OVA-PIC group (Fig. 3A). The total IgG levels increased after the boost on day 21 (Fig. 3B) and 42 (Fig. 3C). All studied nanoparticle formulations and OVA or OVA-poly (I:C) solutions gave similar total IgG responses, except for PLGA-OVA. These nanoparticles showed significant weaker total IgG responses on day 42 and 49, but *co*-encapsulation of poly(I:C) in PLGA nanoparticles increased significantly total IgG titers to similar levels observed with the other nanoparticle suspensions. In conclusion, the nano-

Table 1
Physicochemical characteristics of OVA/poly(I:C) loaded nanoparticles.

Nanoparticles	Size[a] (nm)	PDI[b]	ZP[c] (mV)	EE[d] %		LC[e] %	
				OVA	Poly(I:C)	OVA	Poly(I:C)
PLGA-OVA	157 ± 7	0.060 ± 0.028	-18 ± 1	64.7 ± 4.8	–	6.9 ± 0.5	–
PLGA-OVA-PIC	160 ± 1	0.052 ± 0.019	−22 ± 4	76.7 ± 2.0	13.9 ± 4.2	2.7 ± 0.7	3.0 ± 0.9
Lipo-OVA	124 ± 15	0.152 ± 0.026	44 ± 2	97.0 ± 2.4	–	1.6 ± 0.1	–
Lipo-OVA-PIC	171 ± 9	0.270 ± 0.040	41 ± 1	92.1 ± 5.6	98.6 ± 2.3	1.5 ± 0.1	1.6 ± 0.1
LB-MSN-OVA	656 ± 5	0.280 ± 0.018	−33 ± 3	73.8 ± 5.7	–	15.6 ± 1.2	–
LB-MSN-OVA-PIC	603 ± 17	0.318 ± 0.040	−38 ± 3	34.4 ± 3.3	64.9 ± 14.6	7.9 ± 0.8	5.9 ± 1.3
GNP-OVA	507 ± 31	0.131 ± 0.116	21 ± 2	90.9 ± 14.2	–	4.3 ± 0.7	–
GNP-OVA-PIC	757 ± 235	0.320 ± 0.179	8 ± 12	96.8 ± 4.3	95.0 ± 4.4	3.5 ± 0.9	3.4 ± 1.0

Data are average ± SD of at least 3 independent batches.
[a] Size: Z-average in diameter.
[b] PDI: poly dispersity index.
[c] ZP: zeta potential.
[d] EE: encapsulation efficiency.
[e] LC: loading capacity.

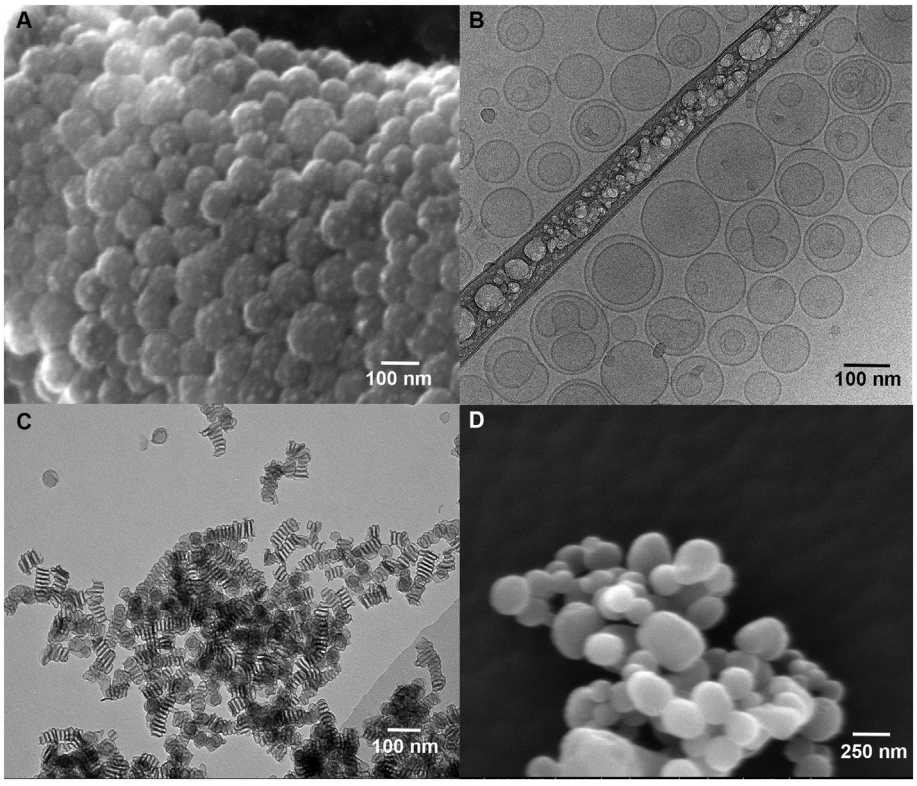

Fig. 1. Electron microscope images of nanoparticles. A) Scanning electron microscopy (SEM) image of PLGA nanoparticles; B) Cryo-EM image of liposomes; C) Transmission electron microscopy (TEM) image of MSNs; D) SEM image of GNPs.

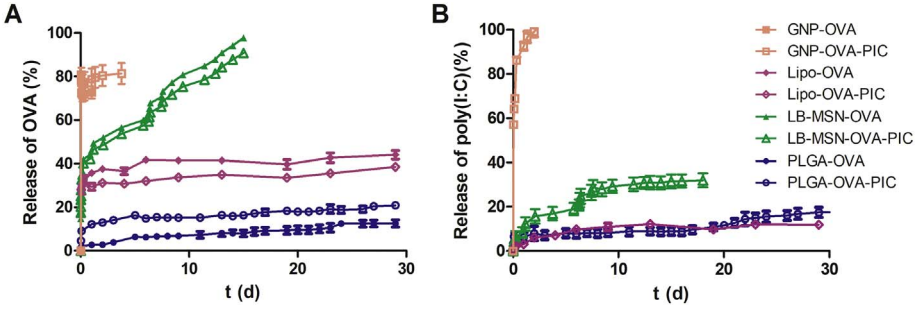

Fig. 2. Release profiles of OVA (A) and poly(I:C) (B) from PLGA nanoparticles (blue/spheres), liposomes (purple/diamonds), MSNs (green/triangles) and GNPs (brown/squares) in PBS at 37 °C. Open and closed symbols correspond to poly(I:C)-containing and poly(I:C)-free nanoparticles, respectively. Data points represent mean ± SD, n = 3. (For interpretation of the references to colour in this figure legend, the reader is referred to the web version of this article.)

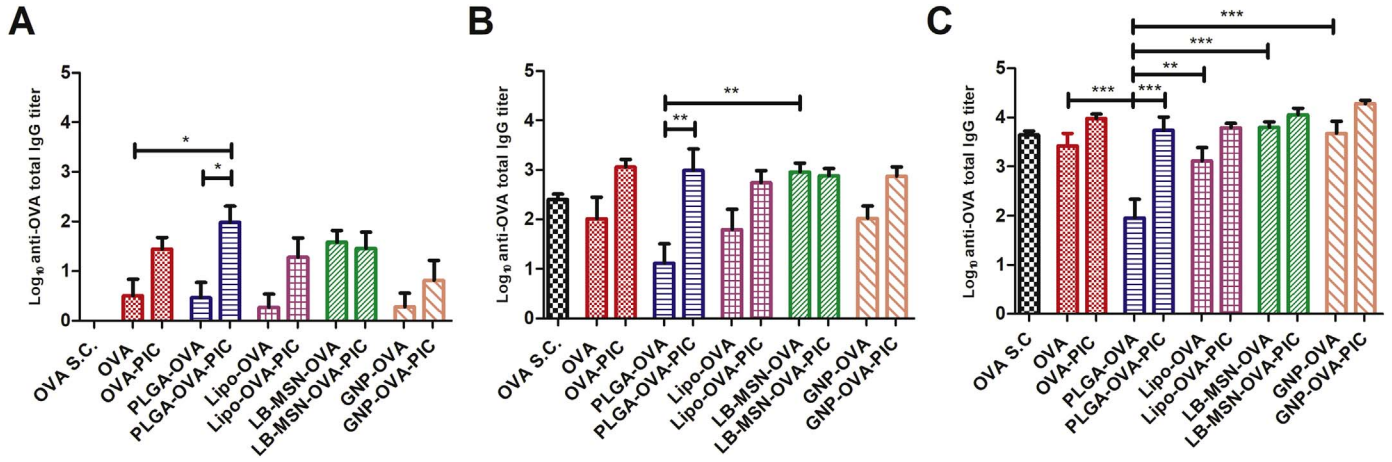

Fig. 3. OVA-specific total IgG antibody titers measured in BALB/c mice on day 21 (A), day 42 (B) and day 49 (C). Bars represent mean ± SEM, n = 8. *p < 0.05, **p < 0.01, ***p < 0.001. All the formulations were injected intradermally, except the subcutaneous control of OVA solution (OVA S.C.). Groups without a bar showed titers below the detection limit of the ELISA.

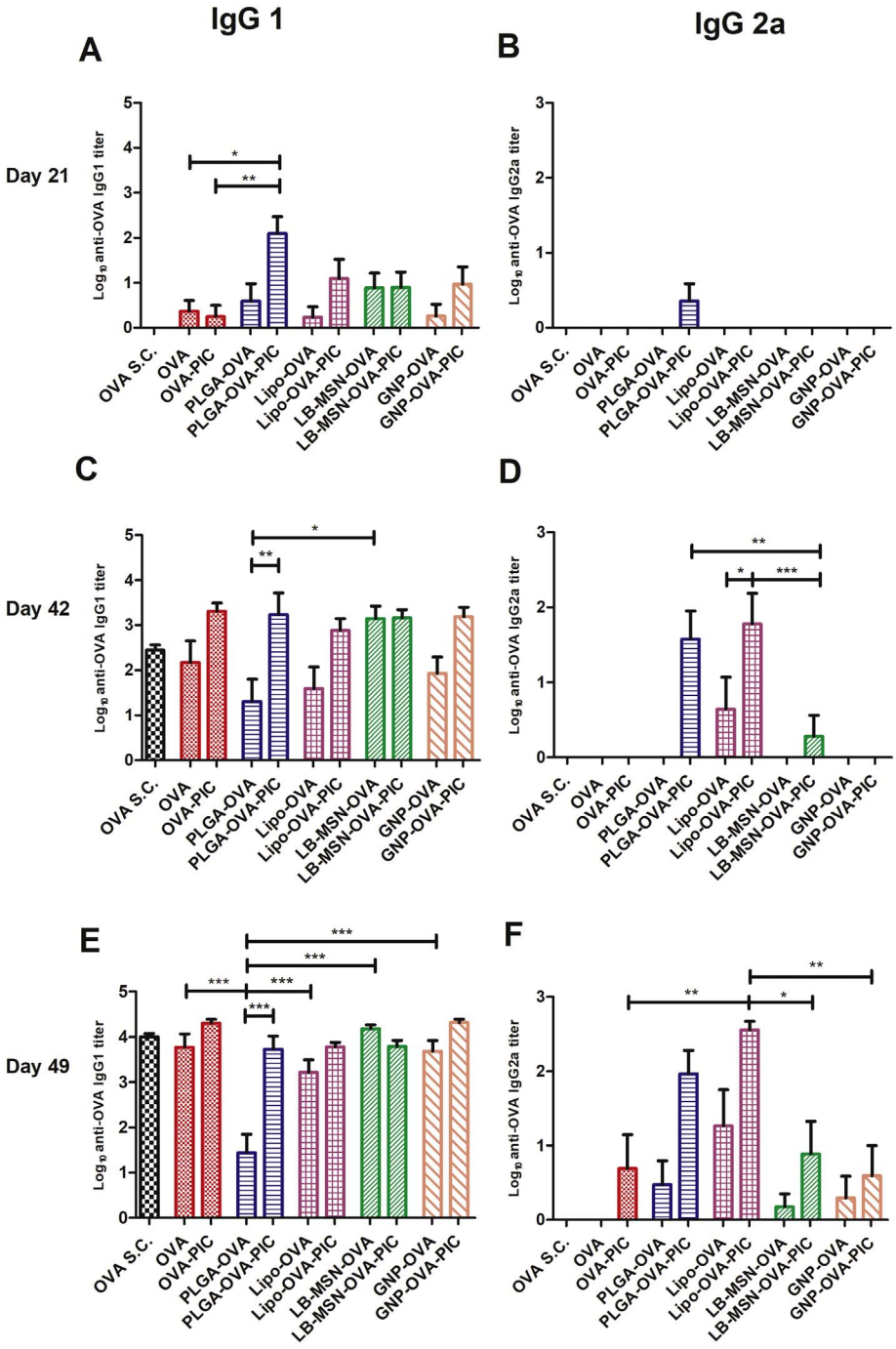

Fig. 4. OVA-specific IgG1 (A, C, E) and IgG2a (B, D, F) antibody titers measured in BALB/c mice on day 21 (A, B), 42 (C, D) and 49 (E, F). Bars represent mean ± SEM, n = 8. *p < 0.05, **p < 0.01, ***p < 0.001. All the formulations were injected intradermally, except the subcutaneous control of OVA solution (OVA S.C). Groups without a bar showed titers below the detection limit of the ELISA.

encapsulation of OVA or *co*-encapsulation of OVA and poly(I:C) did not lead to enhanced total IgG titers.

Next, the subtype IgG1 and IgG2a titers were determined (Fig. 4). The IgG1 titers followed the trend of total IgG titers (Fig. 4A, C, E) and similarly the encapsulation of OVA or *co*-encapsulation of OVA and poly (I:C) did not increase the IgG1 response. However, the encapsulation of OVA, and particularly co-encapsulation of OVA and poly(I:C), strikingly increased the IgG2a response compared to OVA and poly(I:C) solution (Fig. 4B, D, F) (except GNP-OVA-PIC). Furthermore, liposomes and PLGA nanoparticles showed higher IgG2a responses than MSNs and GNPs (Fig. 4F). Specifically, on day 21 only PLGA-OVA-PIC induced an IgG2a response (Fig. 4B). After each boosting on day 21 (Fig. 4D) and 42 (Fig. 4F), there were more groups having an IgG2a response. On day 42, after prime and one boost, all OVA and poly(I:C) co-encapsulated nanoparticles, except GNP-OVA-PIC, showed an IgG2a response (Fig. 4D). After the second boost, on day 49, all the groups, except OVA solution, induced a measurable IgG2a response (Fig. 4F). These results illustrate that encapsulation of OVA, and especially co-encapsulation of OVA and poly(I:C) in nanoparticles is critical for enhancement of IgG2a response but the magnitude of this effect depends on the type of nanoparticles.

3.4. T cell responses after intradermal immunization

The higher IgG2a responses observed with liposomes and PLGA nanoparticles suggested that these formulations may be able to trigger cellular immune responses more effectively. To study the efficacy of the developed nanoparticle formulations to induce T cell mediated immunity *in vivo*, OT-I (OVA specific $CD8^+$ T cells) and OT-II (OVA specific $CD4^+$ T cells) cells were transferred into C57BL/6 mice before

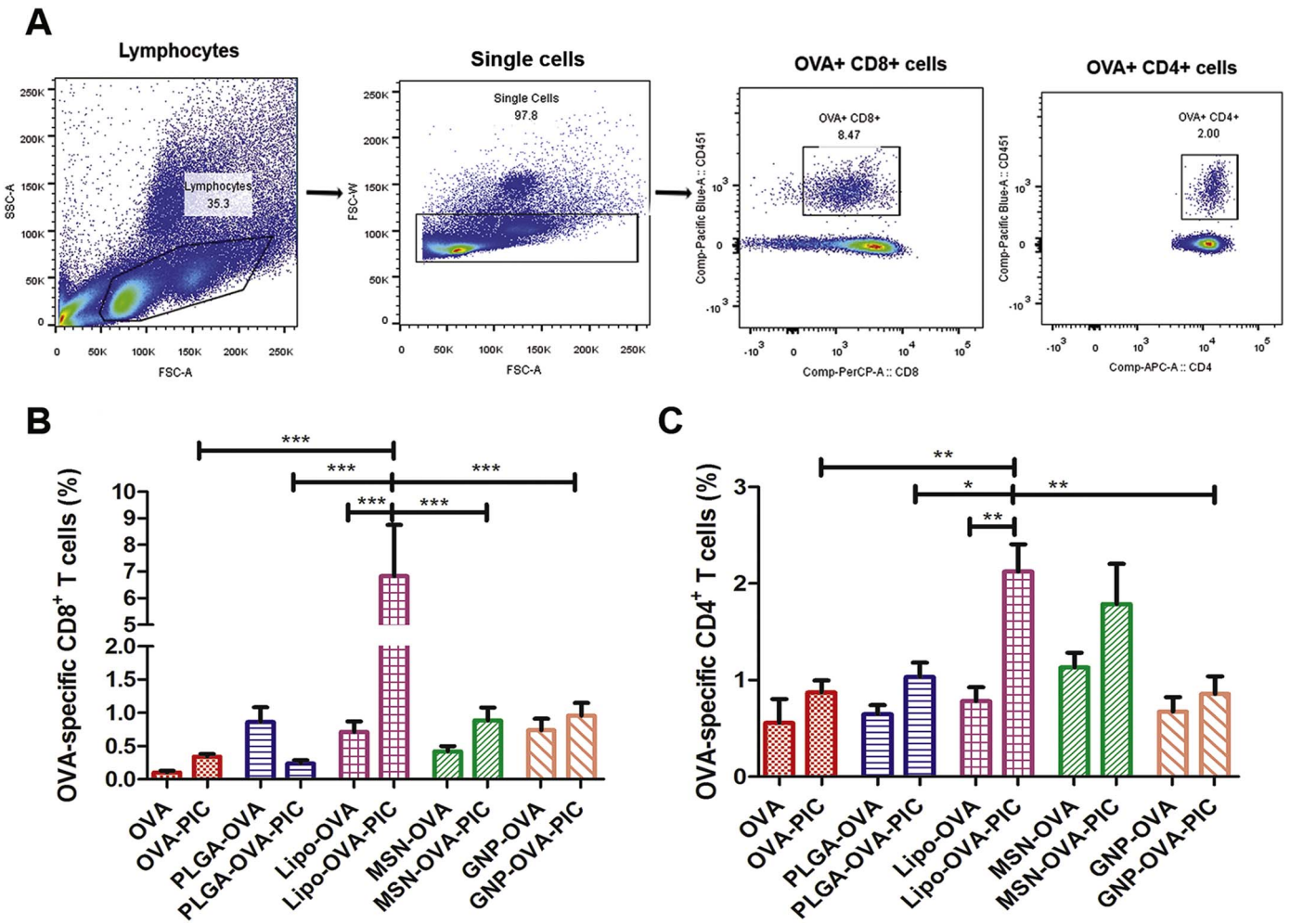

Fig. 5. OVA-specific T cell responses. (A) An example of the flow cytometry gating strategy used to determine the T cell responses. Lymphocytes were gated on forward/sideward scatter, followed by the exclusion of double or adhering cells. After pregating on $CD4^+$ or $CD8^+$ T cells, the percentage of respectively OT-II and OT-I were measured by gating on $CD45.1^+$ cells. OVA specific $CD8^+$ (B) and $CD4^+$ (C) responses of transferred OT-I and OT-II cells in mouse blood 7 days after the immunization (mean ± SEM, n = 5). *p < 0.05, **p < 0.01, ***p < 0.001.

intradermal vaccination. Seven days after the immunization T cell responses in blood were analyzed by flow cytometry with gating strategy shown in Fig. 5A. Lipo-OVA-PIC evoked significant higher $CD8^+$ T cell responses than OVA and poly(I:C) solution and the other nanoparticle formulations (Fig. 5B), suggesting efficient induction of CTL responses by liposomes. In general, nano-encapsulation of OVA or *co*-encapsulation of OVA and poly(I:C) increased the $CD8^+$ response compared to OVA or OVA-poly(I:C) solution. In the case of $CD4^+$ T cell response, Lipo-OVA-PIC and LB-MSN-OVA-PIC induced the strongest response (Fig. 5C). OVA loaded nanoparticles induced similar $CD4^+$ response compared to OVA solution. Poly(I:C) co-encapsulation slightly increased $CD4^+$ responses compared to OVA-loaded nanoparticles but only in the case of liposomes the improvement was significant. Furthermore, the Lipo-OVA-PIC formulation induced a significantly higher $CD4^+$ response than OVA and poly(I:C) solution.

4. Discussion

In recent years, nanoparticles have been intensively investigated as vaccine delivery systems because of their advantages, such as protection of antigen from degradation, increased antigen uptake by dendritic cells and the ability to co-deliver antigen and adjuvant [10,22,41]. Nanoparticles also offer the possibility to adjust the type of immune response by modifying the nanoparticle characteristics such as size, surface charge and antigen release profile [10]. Numerous studies have indicated that nanoparticles can be used to modulate the immune response [9,10,12,15,17,18,20,22,25,39,42]. Owing to its high density of antigen-presenting cells, the skin could be an attractive site of administration of nanoparticulate vaccines. However, relatively little is known about the effect of nanoparticulate vaccines after (microneedle-mediated) intradermal vaccination. Therefore, in this study, we used hollow microneedles together with an applicator to examine the effect of nano-encapsulation of antigen and adjuvant on both the humoral and cellular response in mice. Our results showed that antigen and adjuvant loaded nanoparticles were successfully delivered intradermally in mice by using hollow microneedles together with the applicator, leading to an effective nanoparticle-dependent immune response. Furthermore, after *co*-encapsulation of OVA and poly(I:C) into nanoparticles, the immune response was modulated towards a Th1 direction.

Previously, the in-house developed hollow microneedle/applicator system has been used for immunization with inactivated virus [4–6]. In these studies, we used hollow microneedles with a bore diameter of 20 μm. However, the system has not been used with nanoparticles with larger size (> 100 nm). Therefore, the injection of nanoparticles through the system was tested *in vitro* (data not shown) prior to the *in vivo* studies presented here. These pilot studies showed that the hollow microneedles could be blocked due to occasional nanoparticle aggregation if the bore diameter was 20 μm. By increasing the bore diameter to 50 μm, this problem could be circumvented since increase of the bore diameter decreases particle obstruction in the system.

Consequently, there was no blockage or leakage of formulation during the immunization studies. The success of intradermal injection was confirmed by the formation of a bleb at the injection site after each injection. Furthermore, no adverse effects, such as erythema or skin induration, were observed at the injection site during the studies.

Intradermally administered OVA/poly(I:C) loaded nanoparticles did not increase the total IgG response compared to administration of antigen/adjuvant alone. These results indicate that the encapsulation of OVA or *co*-encapulation of OVA and poly(I:C) is not required for a strong IgG response following intradermal administration. This may be caused by the efficient uptake of the free antigen/adjuvant by antigen-presenting cells in epidermis and dermis (Langerhans cells and dendritic cells) and lymph nodes beneath the skin. Additionally, poly(I:C) has been shown to strongly improve CD8 responses rather than IgG responses [43–45]. In case of PLGA nanoparticles, PLGA-OVA showed even a lower total IgG response than OVA alone. This may be due to a change in the tertiary structure of OVA, either during preparation or in the acidic environment of PLGA nanoparticles during the degradation of the polymer after administration [46,47]. Furthermore, in the current study the OVA dose was much lower (0.31 μg) compared to the dose used in previous studies (*e.g.* ≥ 5 μg) [27,42,48]. The low dose can magnify the detrimental effect of partial OVA degradation in PLGA nanoparticles.

Our results clearly show that co-delivery of the antigen and adjuvant in nanoparticles, increased significantly the IgG2a antibody response compared to OVA/poly(I:C) solution. This indicates that the nanoparticles skewed the immune response of the antigen more towards a Th1 direction [39]. Interestingly, PLGA nanoparticles and liposomes induced higher IgG2a responses than GNPs and MSNs. There are at least two possible underlying factors that may play a role. i) The higher IgG2a response is in line with the slower release of OVA and poly (I:C) from PLGA nanoparticles and liposomes. The sustained release can allow the co-processing of adjuvant and antigen within the same antigen-presenting cell, which is suggested to be crucial for a higher IgG2a response [15,19,22]. Differences in release behavior of OVA/poly(I:C) between the nanoparticles may stem from the differences in the location of the antigen and adjuvant in nanoparticles and in the strength of the interaction between antigen/adjuvant and the nanoparticle matrix. On the one hand, in PLGA nanoparticles and liposomes the antigen/adjuvant is mixed with nanoparticle precursors during synthesis, and the antigen/adjuvant is expected to be localized inside the matrix of PLGA nanoparticles or in the aqueous core layer of liposomes. Therefore, it is likely that the antigen/adjuvant is mostly released after the nanoparticles are taken up and processed by antigen-presenting cells or degraded. On the other hand, with GNPs and MSNs the loading of antigen/adjuvant is done post-synthesis through adsorption of the antigen/adjuvant onto the surface of nanoparticles, presumably based on electrostatic interactions. In addition, in MSNs interactions are expected to occur also between OVA/poly(I:C) and the stabilizing lipid bilayer. Antigen and adjuvant loaded in MSNs and GNPs are sensitive to environmental conditions, such as salts and endogenous proteins present in the skin tissue, that can accelerate the release. As a result, the release of antigen/adjuvant from MSNs and GNPs can be faster than that from PLGA nanoparticles and liposomes, as suggested by the *in vitro* release data. Premature release can consequently lead to separate uptake and processing of antigen and adjuvant by different antigen-presenting cells. ii) The size of PLGA nanoparticles and liposomes (< 200 nm) is substantially smaller than that of MSNs and GNPs (above 500 nm). Although single MSNs had a size below 200 nm, as shown by TEM images [33], DLS showed a larger diameter, indicating the aggregation of MSNs. Smaller particles with a size below 200 nm are expected to be more efficiently taken up by dendritic cells than bigger particles [16]. Moreover, large nanoparticles (500–2000 nm) have been shown to be mostly associated with dendritic cells at the injection site after intradermal delivery, while small (20–200 nm) nanoparticles are able to drain to lymph nodes and target there the dendritic cells [49]. Therefore, the higher IgG2a response induced by the OVA/poly(I:C) loaded PLGA nanoparticles and liposomes could be due to their better uptake by dendritic cells and faster trafficking to the lymph nodes.

As IgG2a levels merely give an indication of the extent of IFN-γ induced isotype switching, we also directly assessed the capacity of each type of nanoparticulate formulation to induce $CD8^+$ and $CD4^+$ T cell responses in OT cell transferred mice. The number of transferred OT cells was kept low as an excess of transgenic T-cells have previously been shown to alter the T-cell response [50]. Our results showed that the Lipo-OVA-PIC formulation showed an exceptional high capacity to induce both $CD8^+$ and $CD4^+$ T cell responses, in line with the data from previous studies [18,48]. The DOTAP based cationic liposomes have been shown to be very effective for the induction of CTL responses [9,12,18], as the cationic lipids promote the activation and maturation of dendritic cells and subsequently the T cell priming. Moreover, EggPC, the main lipid component of the present liposomes, has been shown to facilitate antigen presentation by enhancing peptide binding to MHC class II molecules [51]. So, the superior immune responses of liposomes may be caused by the properties of the lipids.

As explained above, MSNs and GNPs may not be able to enhance the immune response because of their fast release of OVA/poly(I:C) and large size. In case of PLGA-OVA-PIC group, our data showed that the *co*-encapsulation of OVA and poly(I:C) did not increase the T cell responses. This is in contrast to previous reports [12–14], which have shown that the co-encapsulation of OVA and poly(I:C) in PLGA nanoparticles can induce a strong CTL response after intramuscular or subcutaneous vaccination. This indicates that vaccine formulations that provide potent immune responses after intramuscular or subcutaneous administration, may be less suitable for intradermal delivery, re-emphasizing the need for route-specific optimization of vaccine formulations [12,18,42]. Furthermore, targeting of different skin layers may also affect immune responses, as shown in previous studies [52,53]. Nowadays, there is an increasing need of efficient Th1/CTL immune response, for example, in therapeutic vaccinations for cancer [13,17,45] and intracellular pathogens [14,21]. Our results indicate that cationic liposomes are very promising nano-carriers to induce a superior Th1/CTL immune response compared to the other nanoparticles following hollow microneedle-mediated intradermal administration.

5. Conclusions

OVA and poly(I:C) loaded PLGA nanoparticles, liposomes, MSNs and GNPs were successfully developed and compared for hollow microneedle-mediated intradermal immunization in mice. The encapsulation of OVA and co-encapsulation of OVA and poly(I:C) induced a strikingly higher IgG2a antibody response than OVA/poly(I:C) solution, but the type of nanoparticle has a major effect on response. PLGA nanoparticles and especially cationic liposomes induced the highest IgG2a, $CD8^+$ T cell and $CD4^+$ T cell responses, suggesting their superiority for intradermal vaccination. Finally, our study demonstrated that the in house developed hollow microneedle/applicator system is an excellent tool for nanoparticle-based intradermal vaccination and to screen different intradermal vaccine formulations.

Acknowledgements

The research leading to these results has received support from the Innovative Medicines Initiative Joint Undertaking under grant agreement n° 115363 resources of which are composed of financial contribution from the European Union's Seventh Framework Programme (FP7/2007-2013) and EFPIA companies' in kind contribution. G. Du thanks for the part support from Chinese Scholarship Council. Furthermore, we acknowledge K. Pesl for the help with preparation of PLGA nanoparticles and P. Schipper for the help with antibody measurements.

References

[1] N. Li, L.H. Peng, X. Chen, S. Nakagawa, J.Q. Gao, Transcutaneous vaccines: novel advances in technology and delivery for overcoming the barriers, Vaccine 29 (2011) 6179–6190.
[2] K. van der Maaden, W. Jiskoot, J. Bouwstra, Microneedle technologies for (trans) dermal drug and vaccine delivery, J. Control. Release 161 (2012) 645–655.
[3] F.J. Verbaan, S.M. Bal, D.J. van den Berg, J.A. Dijksman, M. van Hecke, H. Verpoorten, A. van den Berg, R. Luttge, J.A. Bouwstra, Improved piercing of microneedle arrays in dermatomed human skin by an impact insertion method, J. Control. Release 128 (2008) 80–88.
[4] K. van der Maaden, S.J. Trietsch, H. Kraan, E.M. Varypataki, S. Romeijn, R. Zwier, H.J. van der Linden, G. Kersten, T. Hankemeier, W. Jiskoot, J. Bouwstra, Novel hollow microneedle technology for depth-controlled microinjection-mediated dermal vaccination: a study with polio vaccine in rats, Pharm. Res. Dordr. 31 (2014) 1846–1854.
[5] P. Schipper, K. van der Maaden, S. Romeijn, C. Oomens, G. Kersten, W. Jiskoot, J. Bouwstra, Determination of depth-dependent intradermal immunogenicity of adjuvanted inactivated polio vaccine delivered by microinjections via hollow microneedles, Pharm. Res. 33 (2016) 2269–2279.
[6] P. Schipper, K. van der Maaden, S. Romeijn, C. Oomens, G. Kersten, W. Jiskoot, J. Bouwstra, Repeated fractional intradermal dosing of an inactivated polio vaccine by a single hollow microneedle leads to superior immune responses, J. Control. Release 242 (2016) 141–147.
[7] M.L. De Temmerman, J. Rejman, J. Demeester, D.J. Irvine, B. Gander, S.C. De Smedt, Particulate vaccines: on the quest for optimal delivery and immune response, Drug Discov. Today 16 (2011) 569–582.
[8] S.G. Reed, M.T. Orr, C.B. Fox, Key roles of adjuvants in modern vaccines, Nat. Med. 19 (2013) 1597–1608.
[9] N. Benne, J. van Duijn, J. Kuiper, W. Jiskoot, B. Slutter, Orchestrating immune responses: how size, shape and rigidity affect the immunogenicity of particulate vaccines, J. Control. Release 234 (2016) 124–134.
[10] T. Akagi, M. Baba, M. Akashi, Biodegradable nanoparticles as vaccine adjuvants and delivery systems: regulation of immune responses by nanoparticle-based vaccine, in: S. Kunugi, T. Yamaoka (Eds.), Polymers in Nanomedicine, 2012, pp. 31–64.
[11] L. Zhao, A. Seth, N. Wibowo, C.X. Zhao, N. Mitter, C.Z. Yu, A.P.J. Middelberg, Nanoparticle vaccines, Vaccine 32 (2014) 327–337.
[12] E.M. Varypataki, A.L. Silva, C. Barnier-Quer, N. Collin, F. Ossendorp, W. Jiskoot, Synthetic long peptide-based vaccine formulations for induction of cell mediated immunity: a comparative study of cationic liposomes and PLGA nanoparticles, J. Control. Release 226 (2016) 98–106.
[13] S. Hamdy, O. Molavi, Z.S. Ma, A. Haddadi, A. Alshamsan, Z. Gobti, S. Elhasi, J. Samuel, A. Lavasanifar, Co-delivery of cancer-associated antigen and Toll-like receptor 4 ligand in PLGA nanoparticles induces potent CD8(+) T cell-mediated anti-tumor immunity, Vaccine 26 (2008) 5046–5057.
[14] C.S.W. Chong, M. Cao, W.W. Wong, K.P. Fischer, W.R. Addison, G.S. Kwon, D.L. Tyrrell, J. Samuel, Enhancement of T helper type 1 immune responses against hepatitis B virus core antigen by PLGA nanoparticle vaccine delivery, J. Control. Release 102 (2005) 85–99.
[15] E. Schlosser, M. Mueller, S. Fischer, S. Basta, D.H. Busch, B. Gander, M. Groettrup, TLR ligands and antigen need to be coencapsulated into the same biodegradable microsphere for the generation of potent cytotoxic T lymphocyte responses, Vaccine 26 (2008) 1626–1637.
[16] M.O. Oyewumi, A. Kumar, Z.R. Cui, Nano-microparticles as immune adjuvants: correlating particle sizes and the resultant immune responses, Expert Rev. Vaccines 9 (2010) 1095–1107.
[17] Y. Fan, J.J. Moon, Nanoparticle drug delivery systems designed to improve cancer vaccines and immunotherapy, Vaccines (Basel) 3 (2015) 662–685.
[18] E.M. Varypataki, K. van der Maaden, J. Bouwstra, F. Ossendorp, W. Jiskoot, Cationic liposomes loaded with a synthetic long peptide and poly(I:C): a defined adjuvanted vaccine for induction of antigen-specific T cell cytotoxicity, AAPS J. 17 (2015) 216–226.
[19] A.L. Silva, R.A. Rosalia, A. Sazak, M.G. Carstens, F. Ossendorp, J. Oostendorp, W. Jiskoot, Optimization of encapsulation of a synthetic long peptide in PLGA nanoparticles: low-burst release is crucial for efficient CD8(+) T cell activation, Eur. J. Pharm. Biopharm. 83 (2013) 338–345.
[20] R.A. Rosalia, L.J. Cruz, S. van Duikeren, A.T. Tromp, A.L. Silva, W. Jiskoot, T. de Gruijl, C. Lowik, J. Oostendorp, S.H. van der Burg, F. Ossendorp, CD40-targeted dendritic cell delivery of PLGA-nanoparticle vaccines induce potent anti-tumor responses, Biomaterials 40 (2015) 88–97.
[21] M. Zaric, O. Lyubomska, O. Touzelet, C. Poux, S. Al-Zahrani, F. Fay, L. Wallace, D. Terhorst, B. Malissen, S. Henri, U.F. Power, C.J. Scott, R.F. Donnelly, A. Kissenpfennig, Skin dendritic cell targeting via microneedle arrays laden with antigen-encapsulated poly-D,L-lactide-co-glycolide nanoparticles induces efficient antitumor and antiviral immune responses, ACS Nano 7 (2013) 2042–2055.
[22] A.M. Hafner, B. Corthesy, H.P. Merkle, Particulate formulations for the delivery of poly(I:C) as vaccine adjuvant, Adv. Drug Deliv. Rev. 65 (2013) 1386–1399.
[23] A.L. Silva, R.A. Rosalia, E. Varypataki, S. Sibuea, F. Ossendorp, W. Jiskoot, Poly-(lactic-*co*-glycolic-acid)-based particulate vaccines: particle uptake by dendritic cells is a key parameter for immune activation, Vaccine 33 (2015) 847–854.
[24] A.L. Silva, P.C. Soema, B. Slutter, F. Ossendorp, W. Jiskoot, PLGA particulate delivery systems for subunit vaccines: linking particle properties to immunogenicity, Hum. Vaccines Immunother. 12 (2016) 1056–1069.
[25] D. Christensen, K.S. Korsholm, P. Andersen, E.M. Agger, Cationic liposomes as vaccine adjuvants, Expert Rev. Vaccines 10 (2011) 513–521.
[26] K.T. Mody, A. Popat, D. Mahony, A.S. Cavallaro, C.Z. Yu, N. Mitter, Mesoporous silica nanoparticles as antigen carriers and adjuvants for vaccine delivery, Nano 5 (2013) 5167–5179.
[27] D. Mahony, A.S. Cavallaro, F. Stahr, T.J. Mahony, S.Z. Qiao, N. Mitter, Mesoporous silica nanoparticles act as a self-adjuvant for ovalbumin model antigen in mice, Small 9 (2013) 3138–3146.
[28] A.O. Elzoghby, W.M. Samy, N.A. Elgindy, Protein-based nanocarriers as promising drug and gene delivery systems, J. Control. Release 161 (2012) 38–49.
[29] M.S. Sudheesh, S.P. Vyas, D.V. Kohli, Nanoparticle-based immunopotentiation via tetanus toxoid-loaded gelatin and aminated gelatin nanoparticles, Drug Deliv. 18 (2011) 320–330.
[30] A.O. Elzoghby, Gelatin-based nanoparticles as drug and gene delivery systems: reviewing three decades of research, J. Control. Release 172 (2013) 1075–1091.
[31] B. Slutter, S.M. Bal, I. Que, E. Kaijzel, C. Lowik, J. Bouwstra, W. Jiskoot, Antigen-adjuvant nanoconjugates for nasal vaccination: an improvement over the use of nanoparticles? Mol. Pharm. 7 (2010) 2207–2215.
[32] A.D. Bangham, M.M. Standish, J.C. Watkins, Diffusion of univalent ions across the lamellae of swollen phospholipids, J. Mol. Biol. 13 (1965) 238–252.
[33] J. Tu, A.L. Boyle, H. Friedrich, P.H. Bomans, J. Bussmann, N.A. Sommerdijk, W. Jiskoot, A. Kros, Mesoporous silica nanoparticles with large pores for the encapsulation and release of proteins, ACS Appl. Mater. Interfaces 8 (2016) 32211–32219.
[34] E.C. Dengler, J. Liu, A. Kerwin, S. Torres, C.M. Olcott, B.N. Bowman, L. Armijo, K. Gentry, J. Wilkerson, J. Wallace, X. Jiang, E.C. Carnes, C.J. Brinker, E.D. Milligan, Mesoporous silica-supported lipid bilayers (protocells) for DNA cargo delivery to the spinal cord, J. Control. Release 168 (2013) 209–224.
[35] J. Tu, G. Du, M. Reza Nejadnik, J. Monkare, K. van der Maaden, P.H.H. Bomans, N. Sommerdijk, B. Slutter, W. Jiskoot, J.A. Bouwstra, A. Kros, Mesoporous silica nanoparticle-coated microneedle arrays for intradermal antigen delivery, Pharm. Res. 34 (8) (2017) 1693–1706.
[36] H. Wang, M.B. Hansen, D.W. Lowik, J.C. van Hest, Y. Li, J.A. Jansen, S.C. Leeuwenburgh, Oppositely charged gelatin nanospheres as building blocks for injectable and biodegradable gels, Adv. Mater. 23 (2011) H119–124.
[37] S. Azarmi, Y. Huang, H. Chen, S. McQuarrie, D. Abrams, W. Roa, W.H. Finlay, G.G. Miller, R. Lobenberg, Optimization of a two-step desolvation method for preparing gelatin nanoparticles and cell uptake studies in 143B osteosarcoma cancer cells, J. Pharm. Pharm. Sci. 9 (2006) 124–132.
[38] K. van der Maaden, S.J. Trietsch, H. Kraan, E.M. Varypataki, S. Romeijn, R. Zwier, H.J. van der Linden, G. Kersten, T. Hankemeier, W. Jiskoot, J. Bouwstra, Novel hollow microneedle technology for depth-controlled microinjection-mediated dermal vaccination: a study with polio vaccine in rats, Pharm. Res. 31 (2014) 1846–1854.
[39] B. Slutter, S.M. Bal, Z. Ding, W. Jiskoot, J.A. Bouwstra, Adjuvant effect of cationic liposomes and CpG depends on administration route, J. Control. Release 154 (2011) 123–130.
[40] A.K. Bajpai, J. Choubey, Design of gelatin nanoparticles as swelling controlled delivery system for chloroquine phosphate, J. Mater. Sci. Mater. Med. 17 (2006) 345–358.
[41] L.J. Peek, C.R. Middaugh, C. Berkland, Nanotechnology in vaccine delivery, Adv. Drug Deliv. Rev. 60 (2008) 915–928.
[42] D. Mohanan, B. Slutter, M. Henriksen-Lacey, W. Jiskoot, J.A. Bouwstra, Y. Perrie, T.M. Kundig, B. Gander, P. Johansen, Administration routes affect the quality of immune responses: a cross-sectional evaluation of particulate antigen-delivery systems, J. Control. Release 147 (2010) 342–349.
[43] H. Mitsui, T. Watanabe, H. Saeki, K. Mori, H. Fujita, Y. Tada, A. Asahina, K. Nakamura, K. Tamaki, Differential expression and function of Toll-like receptors in Langerhans cells: comparison with splenic dendritic cells, J. Invest. Dermatol. 122 (2004) 95–102.
[44] H. Fujita, A. Asahina, H. Mitsui, K. Tamaki, Langerhans cells exhibit low responsiveness to double-stranded RNA, Biochem. Biophys. Res. Commun. 319 (2004) 832–839.
[45] R. Ammi, J. De Waele, Y. Willemen, I. Van Brussel, D.M. Schrijvers, E. Lion, E.L.J. Smits, Poly(I:C) as cancer vaccine adjuvant: Knocking on the door of medical breakthroughs, Pharmacol. Ther. 146 (2015) 120–131.
[46] K. Fu, D.W. Pack, A.M. Klibanov, R. Langer, Visual evidence of acidic environment within degrading poly(lactic-co-glycolic acid) (PLGA) microspheres, Pharm. Res. Dordr. 17 (2000) 100–106.
[47] M. van de Weert, W.E. Hennink, W. Jiskoot, Protein instability in poly(lactic-*co*-glycolic acid) microparticles, Pharm. Res. 17 (2000) 1159–1167.
[48] S.M. Bal, S. Hortensius, Z. Ding, W. Jiskoot, J.A. Bouwstra, Co-encapsulation of antigen and Toll-like receptor ligand in cationic liposomes affects the quality of the immune response in mice after intradermal vaccination, Vaccine 29 (2011) 1045–1052.
[49] V. Manolova, A. Flace, M. Bauer, K. Schwarz, P. Saudan, M.F. Bachmann, Nanoparticles target distinct dendritic cell populations according to their size, Eur. J. Immunol. 38 (2008) 1404–1413.
[50] V.P. Badovinac, J.S. Haring, J.T. Harty, Initial T cell receptor transgenic cell precursor frequency dictates critical aspects of the CD8(+) T cell response to infection, Immunity 26 (2007) 827–841.
[51] R.W. Roof, I.F. Luescher, E.R. Unanue, Phospholipids enhance the binding of peptides to class II major histocompatibility molecules, Proc. Natl. Acad. Sci. U. S. A. 87 (1990) 1735–1739.
[52] C. Liard, S. Munier, M. Arias, A. Joulin-Giet, O. Bonduelle, D. Duffy, R.J. Shattock, B. Verrier, B. Combadiere, Targeting of HIV-p24 particle-based vaccine into differential skin layers induces distinct arms of the immune responses, Vaccine 29 (2011) 6379–6391.
[53] C. Levin, O. Bonduelle, C. Nuttens, C. Primard, B. Verrier, A. Boissonnas, B. Combadiere, Critical role for skin-derived migratory DCs and langerhans cells in TFH and GC responses after intradermal immunization, J. Invest. Dermatol. 137 (9) (2017) 1905–1913.